Observation of Giant Resonance Phenomena in the Two-Step Mechanism of Electron-Xe Collision

M. Takahashi,[1,*] Y. Miyake,[1] N. Watanabe,[1] Y. Udagawa,[1] Y. Sakai,[2] and T. Mukoyama[3]

[1]*Institute of Multidisciplinary Research for Advanced Materials, Tohoku University, Sendai 980-8577, Japan*

[2]*Department of Physics, Toho University, Funabashi 274-8510, Japan*

[3]*Kansai Gaidai University, Hirakata 573-1001, Japan*

(Received 12 July 2006; published 4 January 2007)

We report an $(e, 2e)$ binding energy spectrum of Xe obtained at an impact energy of 2.1 keV, which covers the binding energy range up to 220 eV. The result is directly compared with data from high-energy photoelectron spectroscopy. It is found that an $(e, 2e)$-specific, very broad band appears at around 120 eV, although in other energy regions the binding energy spectra by the two methods are in good agreement. The presence of such a band is revealed for the first time, which can be attributed to the second-order effects of the electron-target interaction that involves giant resonance phenomena of the Xe $4d$ electron.

DOI: 10.1103/PhysRevLett.98.013201 PACS numbers: 34.80.Dp, 32.80.Cy, 32.80.Hd

Ionization processes of rare gases have long been a subject of fundamental importance as well as of interest as a testing ground for many kinds of theoretical models. This is especially true for Xe. In fact, a large number of experimental studies have been conducted for Xe using various methods such as photon-, electron-, and positron-impact ionization cross section measurements [1–3], photoelectron spectroscopy (PES) [4,5], and binary $(e, 2e)$ spectroscopy or electron momentum spectroscopy (EMS) [6–8]. Hence one may want to make comparisons of data by different methods for investigating what can be the common concept in the ionization mechanism, independent of the projectile species. The binding energy spectra by PES and EMS are particularly attractive for the purpose, as they are generally believed to be equivalent, provided the projectile energy is sufficiently high. In this respect attempts at comparison over a wide binding energy range including as many bands as possible are desired, because they make the most stringent assessment.

Indeed such an attempt was made for Xe by Braidwood *et al.* [7]. They measured an EMS binding energy spectrum at high energy-resolution of 1.06 eV full width at half maximum (FWHM) and analyzed it in terms of spectroscopic factor [6], a quantity that corresponds to the square of the amplitude of the single-hole configuration in a final ion state. The results were successfully compared with spectroscopic factors derived from a high-energy PES (HEPES) spectrum by Svensson *et al.* [5] using Al K_α x ray. However, although the HEPES spectrum covers the binding energy range up to 220 eV involving ionization transitions of the valence $5p$, $5s$, and inner shell $4d$, $4p$, $4s$ electrons, the investigation by Braidwood *et al.* [7] was limited to ionization of the valence electrons due to the absence of EMS data above 44 eV. Brunger *et al.* [8] reported an EMS spectrum for the $4d$ electron ionization, but it covers only the specific energy region of 62–74 eV. Clearly, further EMS experiments on Xe are called for, which cover a much wider binding energy range.

In this Letter we report an EMS spectrum of Xe that covers the binding energy range up to 220 eV. The result is compared with the HEPES spectrum of Svensson *et al.* [5] in terms of spectroscopic factor. It is shown that an EMS-specific, very broad band is observed at around 120 eV, although in other energy region the EMS and HEPES spectra are in good agreement. The origin of the band is discussed and identified.

EMS involves coincident detection of the two outgoing electrons produced by electron-impact ionization under the high-energy Bethe ridge conditions [6]. With the aid of the laws of conservation of energy and linear momentum, binding energy of the target electron E_{bind} and recoil momentum of the residual ion $\boldsymbol{q}$ can be determined:

$$E_{\text{bind}} = E_0 - E_1 - E_2, \tag{1}$$

$$\boldsymbol{q} = \boldsymbol{p}_0 - \boldsymbol{p}_1 - \boldsymbol{p}_2. \tag{2}$$

Here the E_j's and $\boldsymbol{p}_j$'s $(j = 0, 1, 2)$ are kinetic energies and momenta of the incident and two outgoing electrons, respectively. The EMS experiment on Xe was carried out at impact energy of 2.1 keV, using a recently developed multichannel $(e, 2e)$ spectrometer [9]. It employs the symmetric noncoplanar geometry where two outgoing electrons having equal energies $(E_1 = E_2)$ and equal polar angles of 45° with respect to the incident electron beam axis are detected. Then the magnitude of $\boldsymbol{q}$ can be determined from the out-of-plane azimuthal angle difference between the two outgoing electrons $\Delta\phi$. The experimental results were obtained by accumulating data at ambient sample gas pressure of 3.0×10^{-4} Pa for 1 month runtime. The instrumental energy and momentum resolution employed were 4.5 eV FWHM and 0.45 a.u. at $\Delta\phi = 0°$.

In Fig. 1(a) we present a $\Delta\phi$-angle integrated EMS spectrum of Xe which was generated by plotting number of the coincidence events as a function of E_{bind}. Vertical bars indicate ionization transition energies of the $5p$-$4s$ electrons [5], showing the $5p^{-1}$-$4s^{-1}$ main bands as well as their satellites. Note that the spectrum above 62 eV is scaled by a factor of 25 to make it easier to see bands due to the inner shell electron ionization. Figure 1(b) shows the HEPES spectrum of Svensson *et al.* [5], which was digitized from the literature.

For EMS and HEPES studies on Xe the distorted-wave impulse approximation (DWIA) [6] and the sudden approximation [10,11] have been widely used. Within these approximations ionization intensities by EMS and PES, I_{EMS} and I_{PES}, can be written as

$$I_{\text{EMS}} \propto S_i^{\alpha} \times |\langle \chi^{(-)}(\boldsymbol{p}_1)\chi^{(-)}(\boldsymbol{p}_2)|\phi_{\alpha}\chi^{(+)}(\boldsymbol{p}_0)\rangle|^2, \quad (3)$$

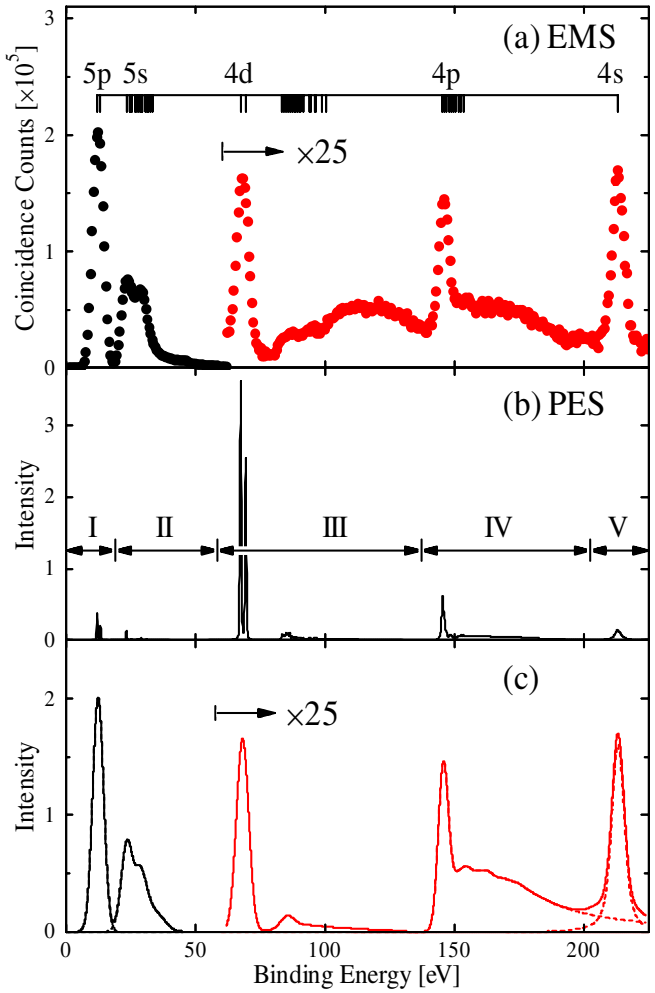

FIG. 1 (color online). (a) EMS spectrum of Xe obtained at an impact energy of 2.1 keV. Note that the spectrum above 62 eV is scaled by a factor of 25. (b) PES spectrum of Xe measured by Svensson *et al.* [5] using Al K_{α} x ray. (c) Results of a least-squares fit to the EMS spectrum. See text for details.

$$I_{\text{PES}} \propto S_i^{\alpha} \times |\langle \phi_{\varepsilon\alpha}|\boldsymbol{r}|\phi_{\alpha}\rangle|^2. \quad (4)$$

Here ϕ_{α} is the normalized Dyson orbital and S_i^{α} is spectroscopic factor for the transition to the ion state i. $\chi^{(\pm)}(\boldsymbol{p})$ are distorted waves for describing the incident and outgoing electrons and $\phi_{\varepsilon\alpha}$ is a continuum wave for the photoelectron. Since the Dyson orbital for a satellite is the same as that for its main band when electron correlation in the target initial state is neglected [6,10,11], Eqs. (3) and (4) tell one that S_i^{α} governs relative intensity of a satellite with respect to its main band in both EMS and HEPES. Note that this is valid as long as one adopts first-order approximation, which assumes the electron projectile to interact with the target only once, such as the plane-wave-impulse and distorted-wave-Born approximations [6] as well as DWIA. Thus it is possible to directly compare the EMS and HEPES spectra in terms of S_i^{α}. For making such a comparison into practice, however, one must take into consideration the difference in the orbital-characteristic nature between the momentum profile $|\langle \chi^{(-)}(\boldsymbol{p}_1)\chi^{(-)}(\boldsymbol{p}_2)|\phi_{\alpha}\chi^{(+)}(\boldsymbol{p}_0)\rangle|^2$ and the square of the dipole matrix element $|\langle \phi_{\varepsilon\alpha}|\boldsymbol{r}|\phi_{\alpha}\rangle|^2$.

In the present study a comparison of the EMS and HEPES spectra was made as follows. First, we cut the HEPES spectrum into five pieces, as indicated by *I*-*V* in Fig. 1(b), so that each piece includes one of the $5p^{-1}$-$4s^{-1}$ main bands and a cluster of satellites at its higher energy. Second, the five pieces were individually folded with the present instrumental energy resolution and the resultant model spectra were subsequently employed as fitting curves to reproduce the EMS spectrum by summing them with appropriate weight factors. This fitting procedure was made based on an assumption that in each piece all the components of a cluster of satellites belong to the same manifold as the main band. For the $5p$ and $5s$ electron ionization or the pieces I and II, the high energy-resolution EMS study of Braidwood *et al.* [7] and theoretical calculations using the configuration-interaction method [12] and the Green's function method [13] are supports of the assumption to a considerable extent. The fit to the EMS spectrum is shown in Fig. 1(c) where the broken lines represent the fitting curves and the solid line their sum.

It can be seen from comparison of Figs. 1(a) and 1(c) that the EMS spectrum, on the whole, is reproduced by the model spectra generated using the HEPES data, except in the energy region of about 100–140 eV where only EMS exhibits substantial intensity; a clear difference between EMS and HEPES is observed here. The good agreement between EMS and HEPES in other energy regions suggests that understanding of the observed difference is beyond the reach of the first-order approximation. Hence one may conceive that possible sources of the difference are multiple scattering effects and/or higher-order effects.

To examine the effects of multiple scattering on the EMS spectrum, we made an additional EMS measurement by increasing the ambient sample gas pressure by a factor

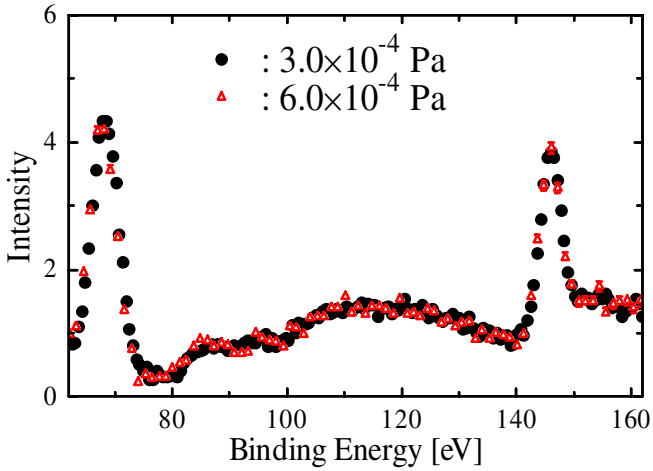

FIG. 2 (color online). Comparison of the EMS spectra of Xe measured at ambient sample gas pressure of 3.0×10^{-4} Pa and 6.0×10^{-4} Pa.

of 2, i.e., experiment at 6.0×10^{-4} Pa. The result is shown in Fig. 2, where the EMS spectrum at 3.0×10^{-4} Pa in Fig. 1(a) is also depicted for comparison. It leaves no doubt that the EMS spectrum does not vary with the ambient sample gas pressure, confirming the present EMS results being free from multiple scattering effects. Thus the following attempt was carried out to make the difference between EMS and HEPES directly visible. First, we searched for additional fitting curves to reproduce the EMS spectrum satisfactorily. Addition of a Gaussian curve centered at 120 eV was eventually found to almost completely reproduce the EMS spectrum, as in Fig. 3(a) where the best fit to the EMS spectrum is shown. Second, we produced a difference spectrum by subtracting the model spectra of the best fit from the EMS spectrum. The result is presented in Fig. 3(b).

The difference spectrum in Fig. 3(b) clearly reveals the presence of a very broad band ($\sim$ 50 eV FWHM) centered at around 120 eV. Such broad nature is strongly reminiscent of giant resonance phenomena [14], in which the $4d$ electron is ionized to the f partial wave due to the double-well potential. As an example, a spectrum by forward-scattering electron energy loss spectroscopy (EELS) is shown in Fig. 3(b), which was generated by transforming optical oscillator strength of Xe [15] using the Bethe-Born conversion factor. Giant resonance profile appears as a broad band ($\sim$ 40 eV FWHM) centered at around 100 eV, and its remarkably large cross section can be recognized by comparing the EELS intensity at 100 eV with that at the ionization potential of the $4d$ electron ($IP_{4d} \approx 69$ eV). It is evident from Fig. 3(b) that the difference spectrum is very similar in shape to the EELS spectrum, while the width of the former is about 10 eV larger than that of the latter. Also evident is that the peak of the former is located at about 20 eV higher energy than that of the latter.

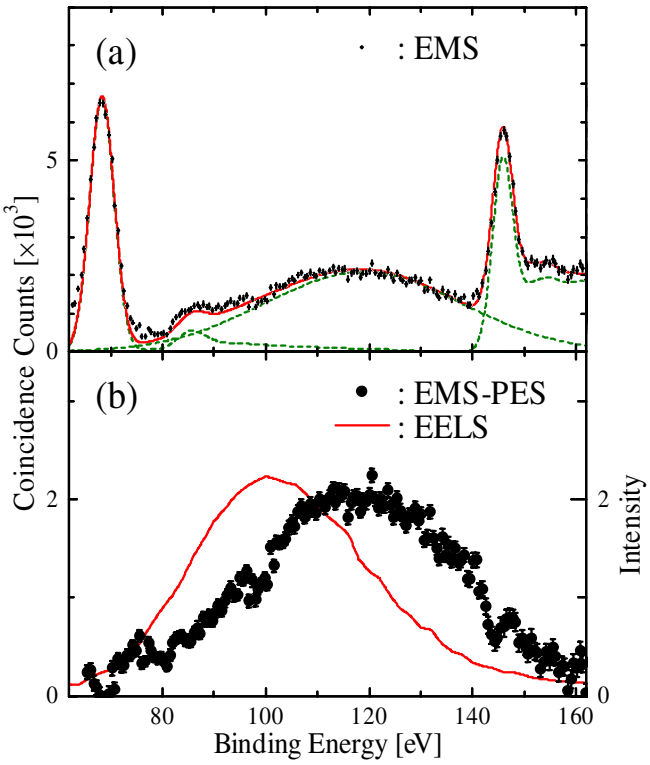

FIG. 3 (color online). (a) Results of a least-squares fit to the EMS spectrum of Xe in the energy region of 62–162 eV. (b) Difference spectrum which was produced by subtracting the model spectra of the fit from the EMS spectrum. The solid line represents an EELS spectrum, which was generated using the optical oscillator strength of Xe [15]. See text for details.

The remaining possible source of the difference between EMS and HEPES can give a rational explanation for the observations above, that is, higher-order effects. Here the two-step (TS) mechanisms [16,17], second-order terms of the plane-wave Born series model [17], hold the key. They involve two successive half-collisions that lead to a joint change of state of two target electrons, and the following processes can contribute to the EMS spectrum:
(a) $e_0 + \mathrm{Xe} \Rightarrow e_1' + e_2 + \mathrm{Xe}^+(5p^{-1}) \Rightarrow e_1 + e_2 + \mathrm{Xe}^{2+}(5p^{-1}, 4d^{-1}) + e(\varepsilon f)$,
(b) $e_0 + \mathrm{Xe} \Rightarrow e_0' + \mathrm{Xe}^+(4d^{-1}) + e(\varepsilon f) \Rightarrow e_1 + e_2 + \mathrm{Xe}^{2+}(5p^{-1}, 4d^{-1}) + e(\varepsilon f)$,
(c) $e_0 + \mathrm{Xe} \Rightarrow e_1' + e_2 + \mathrm{Xe}^+(5s^{-1}) \Rightarrow e_1 + e_2 + \mathrm{Xe}^{2+}(5s^{-1}, 4d^{-1}) + e(\varepsilon f)$,
(d) $e_0 + \mathrm{Xe} \Rightarrow e_0' + \mathrm{Xe}^+(4d^{-1}) + e(\varepsilon f) \Rightarrow e_1 + e_2 + \mathrm{Xe}^{2+}(5s^{-1}, 4d^{-1}) + e(\varepsilon f)$. These TS processes consist of the $(e, 2e)$ ionization process of the $5p$ or $5s$ target electron and the giant resonance process of the $4d$ electron to εf due to a collision with the incident or outgoing electron. Overall contributions of the TS processes can be expressed by the sum of the two components $|f(5p, 4d) + f(4d, 5p)|^2 + |f(5s, 4d) + f(4d, 5s)|^2$, where $f(5p, 4d)$, $f(4d, 5p)$, $f(5s, 4d)$, and $f(4d, 5s)$ represent scattering amplitudes of the processes (a),(b),(c), and (d), respec-

tively. For the process (a) [process (b)] the binding energy in the EMS spectrum is the sum of energy loss in the giant resonance process and ionization transition energy of the $5p$ electron of Xe (Xe^+ with the $4d$ hole), i.e., $E_{\text{bind}} = E_{\text{gr}} + E_{5p}$. The same is true with the processes (c) and (d) if the $5s$ electron is considered instead of $5p$. The giant resonance process involved in the TS processes must be largely dominated by forward scattering under the present experimental conditions where energies of all the incident and outgoing electrons are very high compared with the energy loss. Besides, photoion yield measurements [1] have shown that giant resonance profile of Xe^+ is very similar in both shape and energy to that of Xe. Hence one can take the peak energy of the EELS spectrum in Fig. 3(b) as a representative of E_{gr}, i.e., $E_{\text{gr}} = 100$ eV. Furthermore, for simplicity, let the ionization transition energies of the $5p$ and $5s$ electrons of Xe as well as of Xe^+ be the same as transition energies of the $5p^{-1}$ and $5s^{-1}$ main bands of Xe, i.e., $E_{5p} = IP_{5p} \approx 13$ and $E_{5s} = IP_{5s} \approx 23$ eV. Despite this rather simple treatment of E_{gr}, E_{5p}, and E_{5s}, one can arrive at a surprisingly good agreement with the observations in Fig. 3(b). Namely, the two components, $|f(5p, 4d) + f(4d, 5p)|^2$ and $|f(5s, 4d) + f(4d, 5s)|^2$, are expected to give contributions centered at $E_{\text{bind}} = 113$ and 123 eV to the EMS spectrum, and the average of these values is found very close to the peak energy of the difference spectrum, i.e., $(113 + 123)/2 = 118 \approx 120$ eV. The larger width of the difference spectrum compared with the EELS spectrum can be qualitatively understood by considering the difference in energy between IP_{5p} and IP_{5s}. Clearly, contributions of the TS processes (a)–(d) can account for the difference between EMS and HEPES. We believe that this is the first observation of giant resonance phenomena involved in higher-order effects of the projectile-target interaction.

Finally, it may be worthwhile to discuss why higher-order effects are noticeable in EMS only, though the following process (e), similar to the processes (a) and (c), is possible in PES: (e) $h\nu + \text{Xe} \Rightarrow e' + \text{Xe}^+(5p^{-1} \text{ or } 5s^{-1}) \Rightarrow e + \text{Xe}^{2+}(5p^{-1} \text{ or } 5s^{-1}, 4d^{-1}) + e(\varepsilon f)$. A clue for understanding the reason can be found in Figs. 1(a) and 1(b). The $5p$ and $5s$ electrons dominate total $(e, 2e)$ cross section of Xe over other electrons, whereas the total photoionization cross section is dominated by the $4d$ electron. Let cross sections of the processes (a),(c), and (e) be described as a product of intensities of the two half-collision processes involved. Then, by keeping in mind the remarkably large intensity of giant resonance phenomena [14], one may reach the following conclusion. In EMS intensity of the $5p$ ($5s$) ionization is large, so cross sections of the processes (a) and (c) as well as of the processes (b) and (d) become comparable to the small $(e, 2e)$ cross section for the $4d$ electron. On the other hand, in PES intensity of the $5p$ ($5s$) ionization is small and hence cross section of the process (e) becomes negligibly small compared with the large photoionization cross section for the $4d$ electron.

This research was partially supported by the Ministry of Education, Culture, Sports, Science, and Technology, Grant-in-Aid for Scientific Research (A), No. 16205006, and for Exploratory Research, No. 16654065.

*Electronic address: masahiko@tagen.tohoku.ac.jp

[1] M. Sano, Y. Itoh, T. Koizumi, T. M. Kojima, S. D. Kravis, M. Oura, T. Sekioka, N. Watanabe, Y. Awaya, and F. Koike, J. Phys. B **29**, 5305 (1996).
[2] B.-S. Min, Y. Yoshinari, T. Watabe, Y. Tanaka, C. Takayanagi, T. Takayanagi, K. Wakiya, and H. Suzuki, J. Phys. Soc. Jpn. **62**, 1183 (1993).
[3] G. Laricchia, P. van Reeth, M. Szluinska, and J. Moxom, J. Phys. B **35**, 2525 (2002).
[4] U. Gelius, J. Electron Spectrosc. Relat. Phenom. **5**, 985 (1974).
[5] S. Svensson, B. Eriksson, N. Mårtensson, G. Wendin, and U. Gelius, J. Electron Spectrosc. Relat. Phenom. **47**, 327 (1988).
[6] E. Weigold and I. E. McCarthy, *Electron Momentum Spectroscopy* (Kluwer Academic/Plenum, New York, 1999), and references therein.
[7] S. Braidwood, M. J. Brunger, and E. Weigold, Phys. Rev. A **47**, 2927 (1993).
[8] M. J. Brunger, S. W. Braidwood, I. E. McCarthy, and E. Weigold, J. Phys. B **27**, L597 (1994).
[9] M. Takahashi, N. Watanabe, Y. Khajuria, K. Nakayama, Y. Udagawa, and J. H. D. Eland, J. Electron Spectrosc. Relat. Phenom. **141**, 83 (2004).
[10] T. Åberg, Phys. Lett. A **26**, 515 (1968).
[11] R. L. Martin and D. A. Shirley, Phys. Rev. A **13**, 1475 (1976).
[12] J. P. D. Cook, I. E. McCarthy, J. Mitroy, and E. Weigold, Phys. Rev. A **33**, 211 (1986).
[13] A. S. Kheifets and M. Ya. Amusia, Phys. Rev. A **46**, 1261 (1992).
[14] J. P. Connerade, J. E. Esteva, and R. C. Karnatak, *Giant Resonance in Atoms, Molecules, and Solids* (Plenum, New York, 1986).
[15] W. F. Chan, G. Cooper, X. Guo, G. R. Burton, and C. E. Brion, Phys. Rev. A **46**, 149 (1992).
[16] T. A. Carlson and M. O. Krause, Phys. Rev. **140**, A1057 (1965).
[17] R. J. Tweed, Z. Phys. D **23**, 309 (1992).